A comparative study on thermochemical decomposition of lignocellulosic materials for energy recovery from waste: monitoring of evolved gases, thermogravimetric, kinetic and surface analyses of produced chars

Paulina Copik[1,*], Agnieszka Korus[1], Andrzej Szlęk[1], Mario Ditaranto[2]

[1]Department of Thermal Technology, Silesian University of Technology, Gliwice, Poland

[2]SINTEF Energy Research, Trondheim, Norway

*e–mail: paulina.wienchol@polsl.pl

ABSTRACT

Increased waste generation caused by the growth of urbanisation rate forces scientists and policymakers to rapidly develop and implement optimal waste management strategies. Since there are many ways to waste treatment and each waste material has different physicochemical properties, they should be investigated separately. This paper presents the results of an experimental investigation on the thermal decomposition of the spent coffee grounds (SCG) and textiles under various atmospheres using a vertical tube furnace. In the study, different analytical techniques are used, such as gas chromatography (GC), gas adsorption for surface area and porosity determination, Fourier-transform infrared spectroscopy (FTIR), and thermogravimetric analysis (TGA). Results indicated that SCG sample yielded more calorific pyrolytic gas (209.8 kJ/mol). than TEX (198.7 kJ/mol). O_2/CO_2 atmosphere fasten the fuel decomposition. Concerning biochar, it can be concluded that fast pyrolysis influenced their combustion performance, for

example, its ignition temperature, TEX_slow (475.4 °C) > SGS_slow (470.5 °C) and TEX_fast (469.6 °C) > SGS_fast (415.0 °C), maximum weight loss rates and reactivity. This study will provide a better understanding of thermochemical degradation of waste and allows for developing optimal routes of waste utilisation.

KEYWORDS

municipal solid waste, char, oxy-fuel combustion, gasification, pyrolysis, experiment.

1. Introduction

Due to increasing urbanisation, in the future, most people will inhabit big cities. Metropolises have numerous challenges, including traffic, excessive waste generation, and air and water pollution. Thus, appropriate municipal solid waste (MSW) management is one of the key elements for the sustainable development of urban areas. After recycling, energy recovery from waste is the most favourable method of waste management, in line with the concept of a circular economy. As a result, local governments can reduce greenhouse gas footprints, dispose of waste effectively and create new workplaces [1]–[3]. Besides, the use of waste as a source of energy can decrease fossil fuel depletion and mitigate climate change.

There are plenty of possibilities for extracting energy from waste: for example, via gasification in the presence of sub-stoichiometric air to produce syngas; through pyrolysis, which operates in the absence of oxygen to give various valuable pyrolytic products, such as pyrolytic gas, bio-oil and biochar; and full oxidation (combustion), which allows for heat and electricity production with a reduction in waste volume of up to 90 % [4]. All these methods are generally known as waste-to-energy (WtE) technologies, with incineration currently being the most mature and superior in large-scale applications [5]. Although pyrolysis and gasification are growing in

popularity [6], the variability of feedstock is the main obstacle to fully developing these technologies, since a high degree of pre-treatment is required.

Nevertheless, biochar, which is derived from organic waste pyrolysis, has great potential in environmental and industrial applications owing to its unique physicochemical features [7]. The properties of biochar directly depend on the feedstocks and process conditions employed, which were widely reviewed by Weber and Quicker [8]. Since biochar has desirable fuel properties, such as higher energy density and good grindability, it could potentially be a useful solution where a waste incineration plant could not be deployed close to a city, addressing key issues, including expensive transportation and poor grindability, associated with the direct use of waste as a fuel [9], [10].

Although the incineration sector has evolved over the past decades and the problem of harmful furans and dioxins has been eliminated, there is still an issue regarding carbon dioxide emissions from the part of the carbon contained in the waste that is not of biological origin [2]. Therefore, a step forward in incineration technology development is the implementation of Carbon Capture and Utilisation or Storage (CCUS) techniques in WtE plants, which will lead to negative CO_2 emissions from biogenic carbon in waste, thus decreasing atmospheric CO_2 [11].

Among CCUS technologies, oxy-fuel is considered the most promising method, mostly due to the high partial pressure of carbon dioxide in the flue gas, which results in less energetic carbon capture compared to the post-combustion method [12]. Furthermore, using oxygen instead of air causes the exhaust gas volume to be about five times lower, and thereby gas cleaning is cheaper because fewer materials need to be used to construct an air pollution control system [13]. Since combustion in an oxygen atmosphere also results in a higher process temperature, the

implementation of the oxy-fuel combustion technique in an incineration plant can eliminate the consumption of auxiliary fossil fuel, which is usually used to keep the required temperature [14].

An in-depth understanding of the thermal degradation properties of individual waste materials under various conditions is crucial to provide an optimised utilisation method for municipal solid waste. In the literature, we can find studies of these properties, which are usually product characteristics. Li et al. [15] investigated the bioenergy generation potential of spent coffee grounds (SCG) during pyrolysis at two heating rates of 10 and 60 °C/min using the thermogravimetric technique. The pyrolysis efficiency was estimated at 77–85%, depending on the moisture content of the feedstock. Kelkar et al. [16] used a screw-conveyor pyrolysis reactor to assess the effects of reactor temperature and residence time during the fast pyrolysis on the overall and organic yield of liquid product. Bio-oil production and the effect on its quality of process temperatures ranging from 673 K to 873 K were also investigated by Bok et al. [17]. They found that CO_2 and CO, as well as CH_4 are the three main volatile products during SCG pyrolysis, while in the bio-oils, palmitic and linoleic acids were the dominant compounds, indicating its great potential for further biodiesel production.

Biochar derived from SCG pyrolysis was evaluated by Christou et al. [18] as a soil conditioner for boosting plant growth, while Cho et al. [19] used nano Fe(III) oxide (FO) as an additive material in spent coffee ground (SCG) pyrolysis under a CO_2 atmosphere and investigated its impacts on syngas generation and biochar adsorptive properties. Various researchers have analysed [20]–[22] pyrolysis using CO_2 as a reaction medium in lab-scale reactors. They observed that by using carbon dioxide, the generation of syngas is enhanced, while condensable hydrocarbons (e.g., tar) are reduced. In the most recent study, Primaz et al. [23] used a

thermogravimetric method to study SCG pyrolysis and combustion processes and determine kinetic parameters. Studies on the co-pyrolysis of SCG and other fuels, such as plastics, have also been reported, for example, in [24]. Results indicated that co-pyrolysis improve the performance of the process.

Studies on the pyrolysis and gasification of waste textiles (TEX), such as polyester fiber, cotton, and wool, using thermogravimetric analysis, X-ray diffraction (XRD), and scanning electron microscopy (SEM) were presented in [25], [26]. Tang et al. [27] employed TGA-FTIR analysis to investigate pyrolysis in N_2 and CO_2 atmosphere of six different waste materials, including TEX. The outcomes showed that the growth rate of CO absorbance in CO_2 is significantly faster than in N_2, indicating waste pyrolysis in carbon dioxide can increased the syngas production at higher temperatures.

As the literature reports [28], there are limited studies comparing fast and slow biomass and waste pyrolysis. Up to now, fast and slow pyrolysis of sugarcane bagasse [29], cherry seed [30] and macadamia nutshell [31] have been performed. However, the effect of the heating rate on the physicochemical properties of biochar derived from banana waste and forest residue was reported in two articles [9], [28]. Moreover, no study was found on the combustion characteristics of biochar obtained from fast and slow pyrolysis.

This study is the continuation of our previous research on the thermogravimetric and kinetic analysis of thermal degradation of three different waste materials under various atmospheres, where we retrieved chemical kinetic parameters, such as energy activation (Ea) and pre-exponential factor (A), of pyrolysis and char burnout processes using model-free methods [32]. In this work, we employed the same reaction gases as previously, namely inert (N_2), gasifying

(CO_2) and oxy-combustion (O_2/CO_2); however, we used a laboratory-scale reactor to compare the thermal behaviour of TEX and SCG.

TEX sample was chosen since approximately 113 million metric tons of textile fibers were produced worldwide in 2021. Natural fibers such as cotton or wool had a production volume of 25.4 million metric tons, whereas chemical fibers accounted for the remaining 88.2 million [33]. Over 69% of TEX waste is currently landfilled, which risks soil and groundwater contamination by heavy metals used in the production process [34]. A popular beverage made from roasted coffee beans, coffee is consumed all around the world. The estimated amount of coffee consumed worldwide in 2020 was 167.26 million bags, up 1.9% from the 164.13 million bags recorded in 2019 [35]. Currently, spent coffee grounds have no significant market and hence are problematic for disposal, but their relatively high chemical energy content makes them a potentially valuable feedstock [20]. In the paper, we also prepared waste-derived chars under different pyrolytic conditions and subjected them to further kinetic analysis to evaluate the influence of the size of the sample on the chemical kinetics through a comparison of the kinetic parameters of the char burnout process calculated in a previous paper [32] and within this work. To the best of our knowledge, the combustion properties, as well as kinetic and surface analyses of carbonized SCG and TEX obtained at varied heating rates, have not been widely studied. So, we have focused on a) gas evolution during the thermal degradation of waste materials under different atmospheres to evaluate these materials as energy carriers, and b) biochar properties obtained during fast and slow pyrolysis of used waste samples, which will provide information on the ability of this material for adsorption processes, its reactivity and combustibility, depending on process conditions. This work will contribute the development of studies on waste

thermal conversion processes since it provides new knowledge on waste thermal behaviour as well as essential experimental data, which can be used as an input or for the validation of various mathematical models.

2. Methodology

2.1 Materials

For this study, representative examples of MSW were used, such as TEX and SCG, since they are available worldwide, and their management is considered a common global issue [34]. The detailed characterisation of the materials employed, including proximate and ultimate analyses as well as ash composition analysis, was described in our previous paper [32].

For this study, the chemical composition of the raw material was tested according to the PN-92/P-50092 Standard for plant biomass. The cellulose content was determined by the Seifert method using a mixture of acetylacetone and dioxane, the lignin content using the Tappi method using concentrated sulfuric acid, the holocellulose content using sodium chlorite, and the amount of material soluble in organic solvents by the Soxhlet method. The hemicellulose content was calculated as the difference between that of holocellulose and cellulose. The average results with standard deviations are presented in Table 1.

Table 1. Chemical composition of tested samples

	Extractive substances		Cellulose		Lignin		Hemicellulose		Holocellulose	
Symbol	$\bar{x}$	σ	$\bar{x}$	σ	$\bar{x}$	σ	$\bar{x}$	σ	$\bar{x}$	σ
Unit	%									
SCG	15.5	0.6	18.1	0.4	23.8	0.4	33.4	0.6	51.5	0.5
Tex	3.1	0.2	89.6	0.3	1.6	0.2	9.9	0.6	99.5	0.3

For experimental purposes, samples were cut and ground before the tests down to a size of 0.1 mm. The initial weight of the samples was 2±0.5 g, while the height of the bed was 2 cm.

2.2 Experimental apparatus

2.2.1 Thermochemical degradation process

To investigate the thermal degradation of various waste materials depending on the atmosphere employed, as well as producing chars for further analysis, tests were carried out in a custom-built laboratory-scale experimental rig. The main part of the test rig was a tubular reactor located inside an electrical furnace. Selected gases were introduced into the upper part of the quartz tube reactor. The employed test stand can be used for either a gravimetric or an evolved gas method. The description of the stand and its operation in both modes has been discussed in detail in the article by Korus et al. [36].

In the evolved gas mode, three different atmospheres were used: (a) inert, 100 vol.% N_2, (b) gasifying, 100 vol.% CO_2, and (c) oxidising, 90/10 vol.% CO_2/O_2, with a total flow of 400 ml/min to assess the gas evolution profiles during different processes, such as pyrolysis, gasification and oxy-combustion. The temperature of the process varied from ambient temperature to 800 °C for an inert atmosphere, and to 1100 °C for the other atmospheres, with a constant heating rate of 15 K/min. Afterward, samples were kept in the reactor for a 30 min isotherm at the final temperature for the given atmosphere. Gas samples were taken at 90 s intervals and analysed post-run with GC-TCD. Each experiment was replicated to evaluate the reproducibility of the results. The temperature of the sample was registered with a thermocouple inserted into the reactor, and the mean value was reported for each sampling interval.

In the fast pyrolysis experiment, only inert conditions were employed. The sample was placed into a crucible attached to the rod, while the furnace panel was in the upper position so that the reactor was above the sample holder. A high heating rate of ca. 1700 °C/min was achieved by lowering the furnace, which was pre-heated up to 800 °C and constantly purged with N_2, so that it rapidly enclosed the sample that was waiting in the ambient atmosphere.

Apart from the lab-scale test stand, the SCG char was also produced in a muffle furnace by inserting a crucible with a lid (dedicated to volatile matter analysis) containing a 2 g sample into a furnace heated to 800 °C for 7 minutes.

Due to the small amount of the sample, the collection and analysis of the liquid products were not feasible. Thus, we calculated the percentage of liquids by the difference in weights and assumed that they contained volatile organic compounds and water vapour.

2.2.2 Gas sampling and analysis

To evaluate the effect of the atmosphere on the gaseous products during thermal decomposition, gases were captured into gas bags behind the reactor at 90 s intervals, during degradation processes. To analyse the gathered gas, a gas chromatograph (Agilent 6890N) was used, which detected six different gases (CO_2, CO, CH_4, H_2, N_2 and O_2). The conditions for the analysis of the gaseous products have been presented in detail in the study of Korus et al. [37].

2.3 Characterisation of solid products

2.3.1 Thermogravimetric analysis

Thermal degradation under oxy-fired conditions of the obtained chars was carried out at standard atmospheric pressure using a TGA/DSC analyser (Netzsch STA 409 PC Luxx) with a sensitivity of 0.001 mg and an accuracy of 1 % of the measurement range.

Before each experiment, samples were dried for 2-3 h at 105 °C to remove moisture. To avoid heat and mass transfer limitations, the initial weight of the samples was 5 mg. Sample mass loss profiles were determined based on dynamic heating runs, with a linear temperature increase from 100 to 1000 °C at heating rates (β) of 5, 10 and 15 K/min. All the experiments were performed under an oxy-combustion atmosphere with a total flow rate of 100 ml/min, with 10 % oxygen and 90 % carbon dioxide, using 30 ml/min nitrogen as a purge gas. Blank experiments were carried out to obtain the baselines, used to subtract the buoyancy effect, calibrating the experiments with samples.

The obtained TG and DTG curves were used to evaluate the parameters of char oxy-combustion, such as the temperature at which the fuel sample starts to burn, which is known as the ignition

temperature (T_i), the temperature at which sample combustion is completed, which is the burnout temperature (T_f) and the maximum peak temperature (T_p). T_i was determined by the tangent method described in [38], T_f was defined as the temperature at which the combustion rate decreases to 1 wt.%/min at the end of the combustion process [39], and T_p represented the temperature corresponding to the peak of the DTG profile.

The characteristic temperatures were correlated with various combustibility indexes such as the ignition index (D_i), which refers how quickly or slowly the fuel was ignited, the burnout index (D_f), and the combustion indexes, such as S, H_f and C given by Mureddu et al. [40] (Eq. 1-5).

$$D_i = \frac{DTG_{max}}{t_p t_i} \tag{1}$$

where DTG_{max} is the maximum combustion rate, t_p is the corresponding time of the maximum peak, and t_i is the ignition time.

$$D_f = \frac{DTG_{max}}{\Delta t_{1/2} t_p t_f} \tag{2}$$

where $\Delta t_{1/2}$ is the time range for $\frac{DTG}{DTG_{max}} = 0.5$ and t_f is the burnout time.

The S index reflects the ignition, combustion, and burnout properties of a fuel. The larger the value of the S index, the higher the combustion activity is.

$$S = \frac{DTG_{max}\, DTG_{mean}}{T_f T_i^2} \tag{3}$$

where DTG_{mean} represents the mean combustion rate.

H_f describes the rate and intensity of the combustion process. The smaller the value of the H_f index, the better the combustion properties are [41].

$$H_f = T_p ln\left(\frac{\Delta T_{1/2}}{DTG_{max}}\right) \quad (4)$$

C is the flammability index, which is described as:

$$C = \frac{DTG_{max}}{T_i^2} \quad (5)$$

These indicators are widely used for the evaluation of the combustion performance of different fuels, for example, coal [42], [43], biomass [40], [44], and hydrochars [45].

2.3.2 Kinetic analysis

The results of thermogravimetric analysis at various heating rates were also used to calculate the kinetic parameters. In this study, an isoconversional approach to solid-state kinetics was employed, which allowed kinetic data to be retrieved, i.e., activation energies, E(α), and then, pre-exponential factors, A(α), without any knowledge of the reaction model. A detailed description of model-free methods can be found in [32], [46]–[48]. In this study, differential Friedman, as well as integral Vyazovkin techniques, were used. All the calculations within the presented study were performed with Netzsch Kinetics Neo software (v.2.5.0.1) supported with MS Excel software. Friedman and Vyazovkin analyses were conducted as implemented in the Netzsch software, with a results resolution of 0.01 for α.

2.3.3 Porosity and surface analysis

The surface area and pore size distribution (PSD) of the residual chars created during feedstock conversion under the inert atmosphere were calculated using dual two-dimensional non-local density functional theory (2D-NLDFT) models developed by Jagiello and Olivier [49], for N_2 adsorption at 77 K and CO_2 adsorption at 273 K. Isotherms were collected with a Micromeritics

TriStar II 3020 analyser. The N_2 isotherm provided insight into the mesopores, while the CO_2 adsorption accounted for the micropores < 10 Å. The PSD calculations were performed using the SAIEUS software that allows the simultaneous fitting of two measured isotherms with the respective theoretical kernels [50]. Additionally, specific surface area calculated with classical Brunauer–Emmett–Teller (BET) method using N_2 isotherm was provided as the reference.

Attenuated total reflectance Fourier transform infrared spectroscopy (ATR-FTIR) was used to examine the surface of the residues from the TEX and SCG decomposition. Spectra constructed from 32 scans, with a resolution of 4 cm^{-1} within the range of 4000-700 cm^{-1} wavenumbers were taken with a Perkin Elmer Spectrum 100 spectrometer. Two repetitions were made for each sample and the averaged spectra are reported herein.

3. RESULTS AND DISCUSSION

3.1 Thermal degradation process

3.1.1 Effect of the atmosphere on product distribution

Firstly, the product distribution after the pyrolysis, gasification and oxidation experiments described in section 2.2.1 was calculated for both samples, as shown in Figure 1. After the slow pyrolysis process, the solid phase accounted for 21% and 10% of the SCG and the TEX samples, which were in agreement with a proximate analysis of the used samples presented in [32], which means that all volatile matter have been released from the samples and only char remains. The gaseous phase was around 17% and 12% for SCG_slow and TEX_slow after the pyrolysis process. The remaining mass was assumed to converted into the liquid products and for both

samples, it was the largest part. Similar findings for pyrolysis of lignocellulosic materials can be found in several articles, for example, [51], [52].

In gasifying and oxidising atmospheres, a larger share of gaseous products, a smaller part of liquid yield, and a lack of solid phase can be observed than in the inert atmosphere, suggesting complete conversion of char as well as secondary reactions of tar. According to Yue et al. [53], it was caused by the fact that more cracking reactions occurred and more oxygen-containing functional groups (i.e. carbonyl group) were produced when CO_2 was present. Oxygen-containing functional groups were easier to combine with the hydrogen radical producing water, which involved in gasification with char, resulting in the decreasing of liquid phase yield.

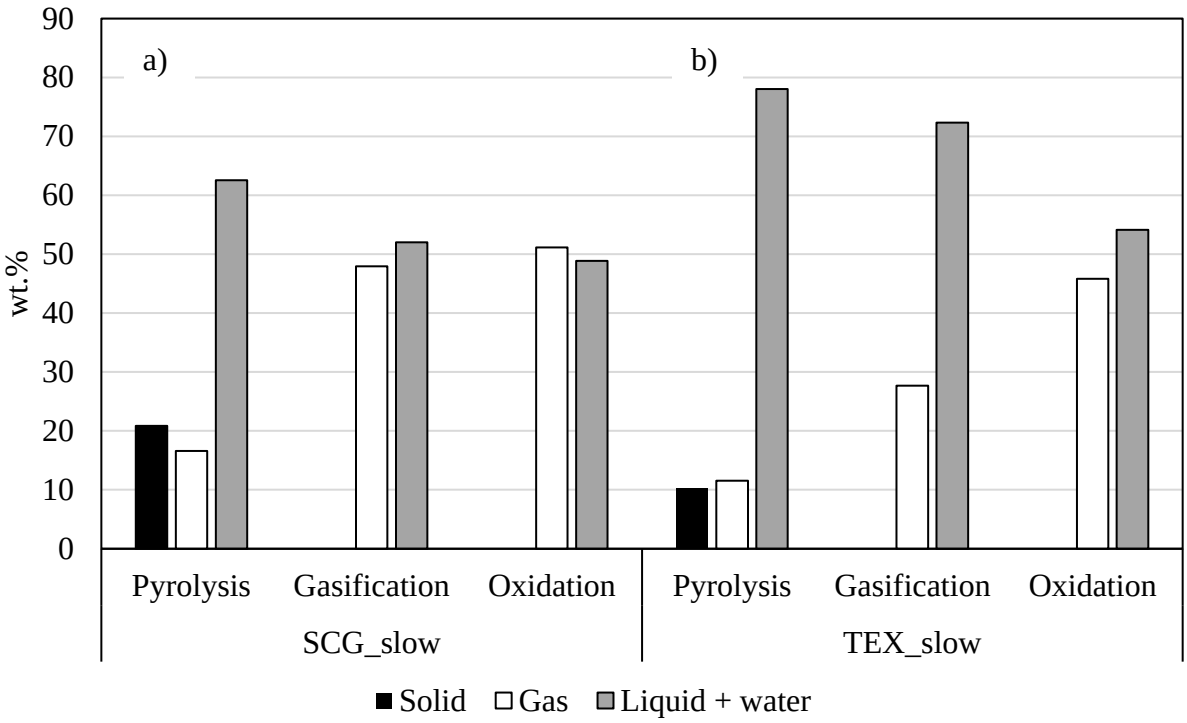

Figure 1 Product distribution after tests under different atmospheres using a) SCG and b) TEX samples

3.1.2 Effect of the atmosphere on gaseous products

Gas evolution profiles during the thermal degradation of TEX and SCG under different conditions are presented in Figures 2-4. For TEX pyrolysis, the evolution of three gases, namely CO_2, CO and CH_4, was registered. Since during the gasification and oxidation tests, CO_2 was consumed rather than produced, it was not reported in this article. Although a small amount of H_2 could also be observed in the chromatograms from TEX decomposition, the concentrations were below the limit of quantification (3000 ppm), and thus they were not presented in this study. It is plausible that some heavier hydrocarbons, such as acetylene and ethylene, were formed as well, yet the instrumental methods applied for the analysis did not allow their detection. The yields of H_2 from the thermal degradation of SCG were high enough to be quantified and reported.

To assess the reproducibility of the results from both experiments, the standard deviation was calculated and presented in graphs. As can be seen, the values of CO, CH_4 as well as CO_2 (in the case of the inert atmosphere) are consistent, meaning that the tests were carried out correctly and that the selected methodology was appropriate. There was a slight discrepancy in the case of hydrogen production, which may be the result of its low level in the sample. However, after integrating the area under the curve, the values of the hydrogen formed during both experiments are similar, namely 1.9 mmol and 2.2 mmol.

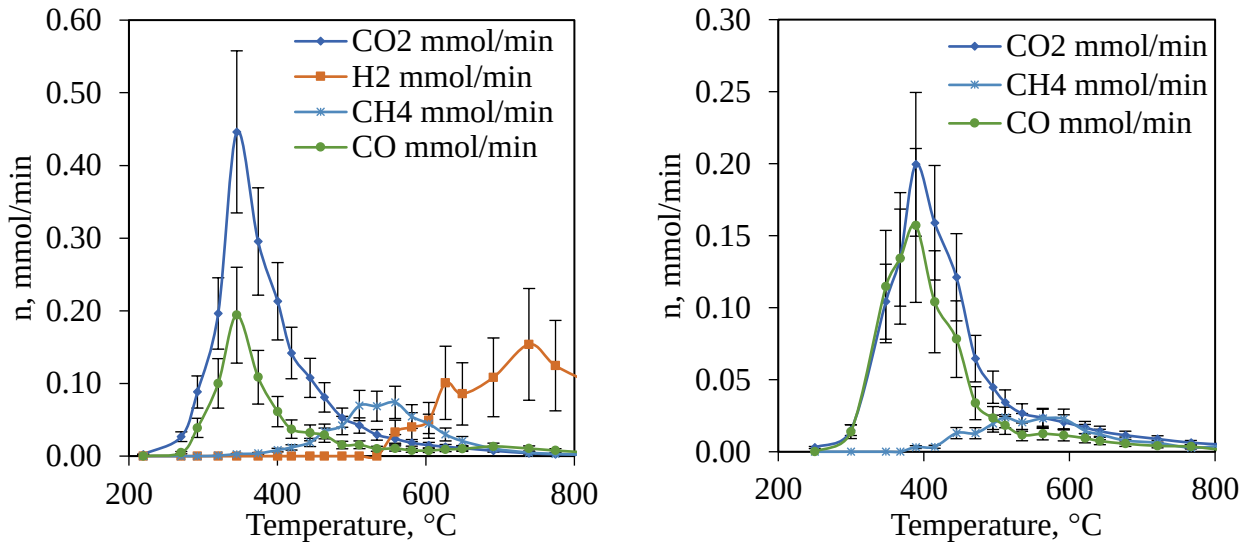

Figure 2. Gas evolution during the thermal degradation of a) SCG and b) TEX under N_2 atmosphere

Comparing the inert and gasifying atmospheres, it was observed that below 600 °C, there were no significant differences in the gaseous products. In both atmospheres, the maximum peak of CO was around 0.15 mmol/min and appeared at 380 °C (TEX) and 0.20 mmol/min at 350 °C for SCG, while the CH_4 peak height is of 0.03 mmol/min and occurred at 550 °C for TEX, and 0.07 mmol/min at 560 °C for SCG. However, in the gasifying atmosphere, a second peak of CO could be distinguished above 700 °C with a height of 2.5 mmol/min (TEX) and 5.8 mmol/min (SCG), which resulted from the Boudouard reaction of char with CO_2 (Eq. 6). Similar findings were reported in [54], [55].

$$C+CO_2 \leftrightarrow 2CO \quad (6)$$

For both the examined materials, the mechanism of devolatilization was not changed by the switch of the atmosphere from inert to gasifying, as revealed by the similarities in the intensity and temperature range of the CH_4 and the first CO peaks. For TEX, the ratio of carbon evolved as CH_4

and CO generated during devolatilization in N_2 and CO_2 was equal to 0.89 and 0.83. While for SCG, it was 0.73 and 0.75, for CH_4 and CO, respectively. These results could indicate that the amount of CO_2 produced during the volatiles release process in the gasifying atmosphere was also comparable to that obtained during pyrolysis in an inert atmosphere. The amounts of carbon released in the later stage of gasification, where the gasification of the solid residue occurred, corresponded to the amount of char recovered from the reactor after the pyrolysis, i.e., 10 % for TEX and 20 % for SCG. This observation corroborated the finding that similar yields of volatiles were released from the samples during their devolatilization in N_2 and CO_2.

The observed differences in the CH_4 and H_2 yields from the two materials could have been caused by their structural differences (Table 1). These gases were formed in the later stage of the devolatilization process and were most likely the result of the secondary reactions between the primary char and the primary volatiles adsorbed on its surface. At sufficiently high temperatures, the volatiles underwent polymerisation, forming H_2 during the dehydrogenation of the aromatic rings. Meanwhile, functional groups were released from the substituted compounds in the form of methane and some light hydrocarbons. Substantial quantitative and qualitative differences in the volatiles released from the TEX and SCG could be expected. The TEX sample is composed mainly of cellulose, and its decomposition during the primary pyrolysis consisted of two possible pathways: a) depolymerization to anhydro-oligosaccharides, monomeric anhydrosugars and their derivatives, which formed the majority of the char, and b) pyranose ring scission to light species, including H_2O, CH_4, CO and CO_2 [56]–[58]. On the other hand, SCG comprises hemicellulose and lignin along with the cellulose constituent. Hemicellulose, the most labile compound, is a matrix of polysaccharides, while lignin, the most thermally stable, comprises highly interconnected and cross-

linked p-hydroxyphenyl, syringyl and guaiacyl units [59]. The more complex structure of SCG likely resulted in a higher yield of the heavy and highly substituted compounds, resulting in the more intense release of H_2 and CH_4 from the secondary reactions of the volatiles.

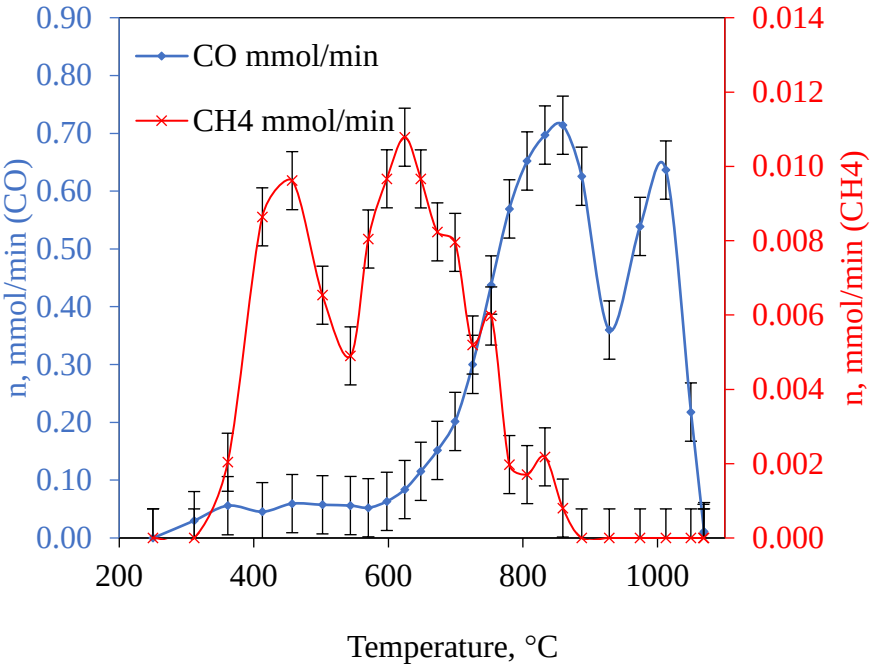

(a)

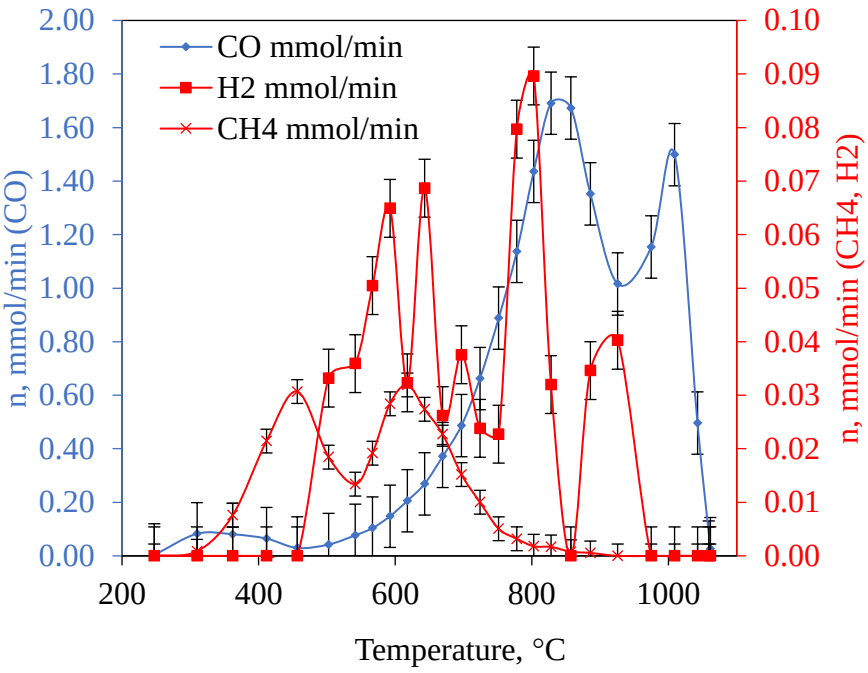

(b)

Figure 3. Gas evolution during the thermal degradation of a) TEX and b) SCG under CO_2 atmosphere

In the oxidising atmosphere, most gases were released over a temperature range of 300 to 550 °C due to the presence of highly reactive oxygen, which can be observed in Figure 4. The peaks of CH_4 and CO corresponded to the highest oxygen uptake, i.e. 85 % for TEX and 95 % for SCG. In this atmosphere, the formation of CH_4 occurred at the same temperature as the initial CO and CO_2 release. These results suggested that differences occurred in the devolatilization of the samples in the presence of oxygen. In the inert conditions, methane and hydrogen were produced at higher temperature (above 500 °C) due to the secondary reactions of tars adsorbed on the char (demethylation and dehydrogenation), whereas, when oxygen was supplied, the tars underwent homogenous reactions with O_2 immediately after their release from the sample, i.e., at temperatures of around 300 °C. Tar decomposition in the gas phase resulted in the loss of functional groups, releasing CH_4, and ring opening reactions, which yielded CO and CO_2, significantly increasing the molar flows of these compounds. No H_2 was detected in the oxidation tests of both samples as it was instantaneously combusted to H_2O.

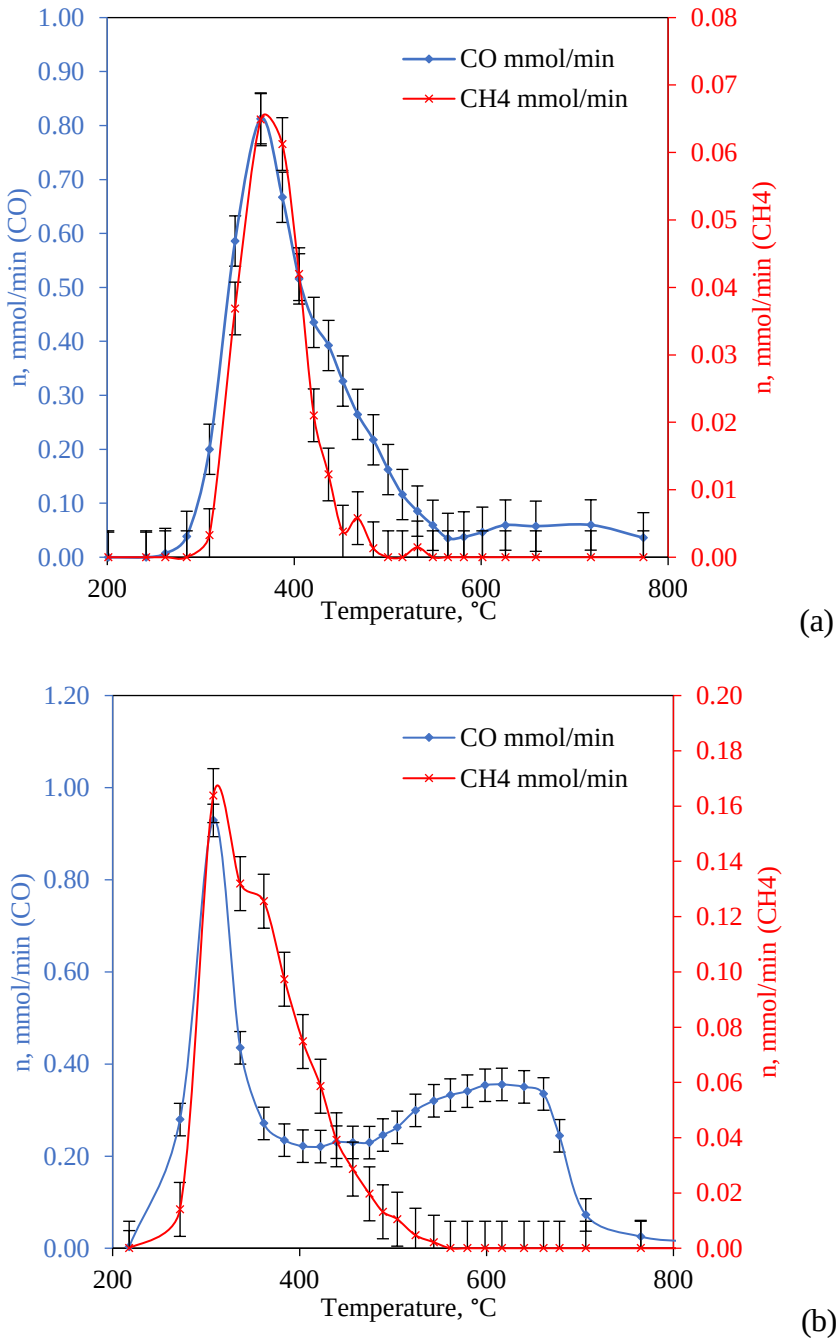

Figure 4. Gas evolution during the thermal degradation of a) TEX and b) SCG under O_2/CO_2

atmosphere

The pyrolytic gas composition from SCG and TEX pyrolysis is presented in Figure 5. The results indicated that gas produced during the SCG pyrolysis contained more hydrogen and methane, and thus it had a slightly higher value of LHV, namely, 209.8 kJ/mol. For TEX pyrolysis, the LHV of the pyrolytic gas was 198.7 kJ/mol.

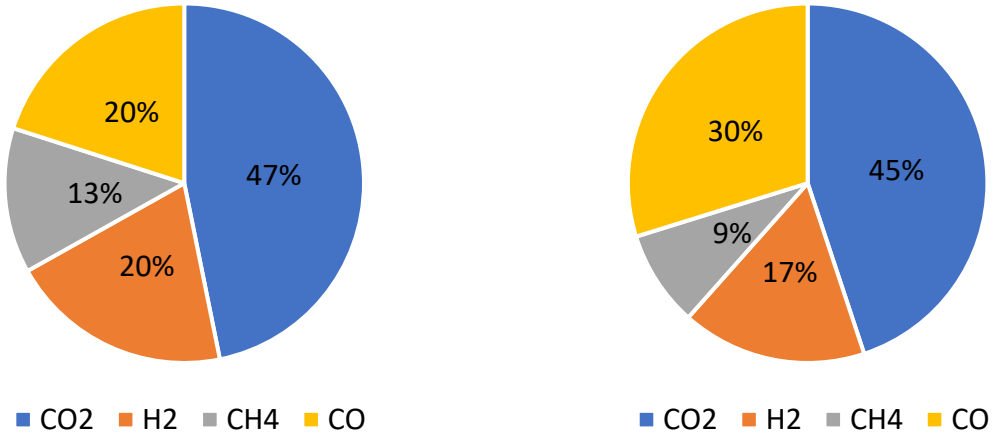

(a) (b)

Figure 5. Composition of the pyrolytic gas for a) SCG and b) TEX sample

3.1.3 Effect of the reaction atmosphere on the solid residue

Figure s 6 and 7 show the solid residue after the experiments. In the N_2 atmosphere, char was formed with a mass of 10% and 20% of the initial weight of the TEX and SCG, respectively. The higher weight of solid residue generated during spent coffee grounds pyrolysis can be ascribed to the occurrence of lignin in the sample, which contributes to char formation [55],[27], [60]. Under gasifying and oxidising conditions, the solid residue comprised only a small amount of ash and thus it was not quantified. Visual examination of the residues formed under the CO_2 atmosphere

suggested complete char gasification, which correlates with the similar amounts of carbon released during gasification and combustion tests (Figure 1). Thus, it is presumed that the solid residue is almost ash. Similar findings were observed in [27], [60]. Over 4 times higher ash content in SCG, compared with textiles as reported in [32], resulted in a more abundant residue from the gasification and combustion of this sample. The different colours of the gasification and combustion residues might result from the different form of inorganic compounds, as CO_2 is a weaker oxidising agent than O_2. Under the oxidising atmosphere, the resulting ash took a greenish colour, which could be explained by the existence of silicates, such as magnesium iron silicate with the chemical formula $(Mg, Fe)_2SiO_4$ or by the occurrence of iron (Fe) and sulphur (S) in the ash, which under the influence of high temperature formed iron sulphide [61]. Nevertheless, research on produced ash under oxy-MSW combustion should be further investigated.

(a) (b) (c)

Figure 6. Solid residue after thermal degradation of textiles under a) inert, b) gasifying and c) oxidising conditions

(a) (b) (c)

Figure 7. Solid residue after thermal degradation of coffee grounds under a) inert, b) gasifying and c) oxidising conditions

The ATR-FTIR spectra of each residue are presented in Figure 8. The pyrolytic chars had a very poorly developed spectra, suggesting a high level of the graphitisation, with barely visible increase in absorption around 1600 and 1000 cm^{-1}, plausibly from some residual C=O and C-O structures, respectively. The spectra of the gasification residues were relatively flat, the increased band at 1000 cm^{-1} in the solids obtained from SCG gasification most likely arose from the presence of quartz wool residue that contaminated the sample, as its powdered form did not allow for clean removal from the wool plug.

The most interesting spectra were observed for the ash from oxidation tests; the residue from the textiles had an especially pronounced absorption around the 1000 cm^{-1} suggest high content of SiO_2 [62], corroborating the TEX ash composition analysis [32]. The bands at 1600 and 1390 cm^{-1} in the SCG residue likely result from the K_2O [63], the main compound of the SCG ash.

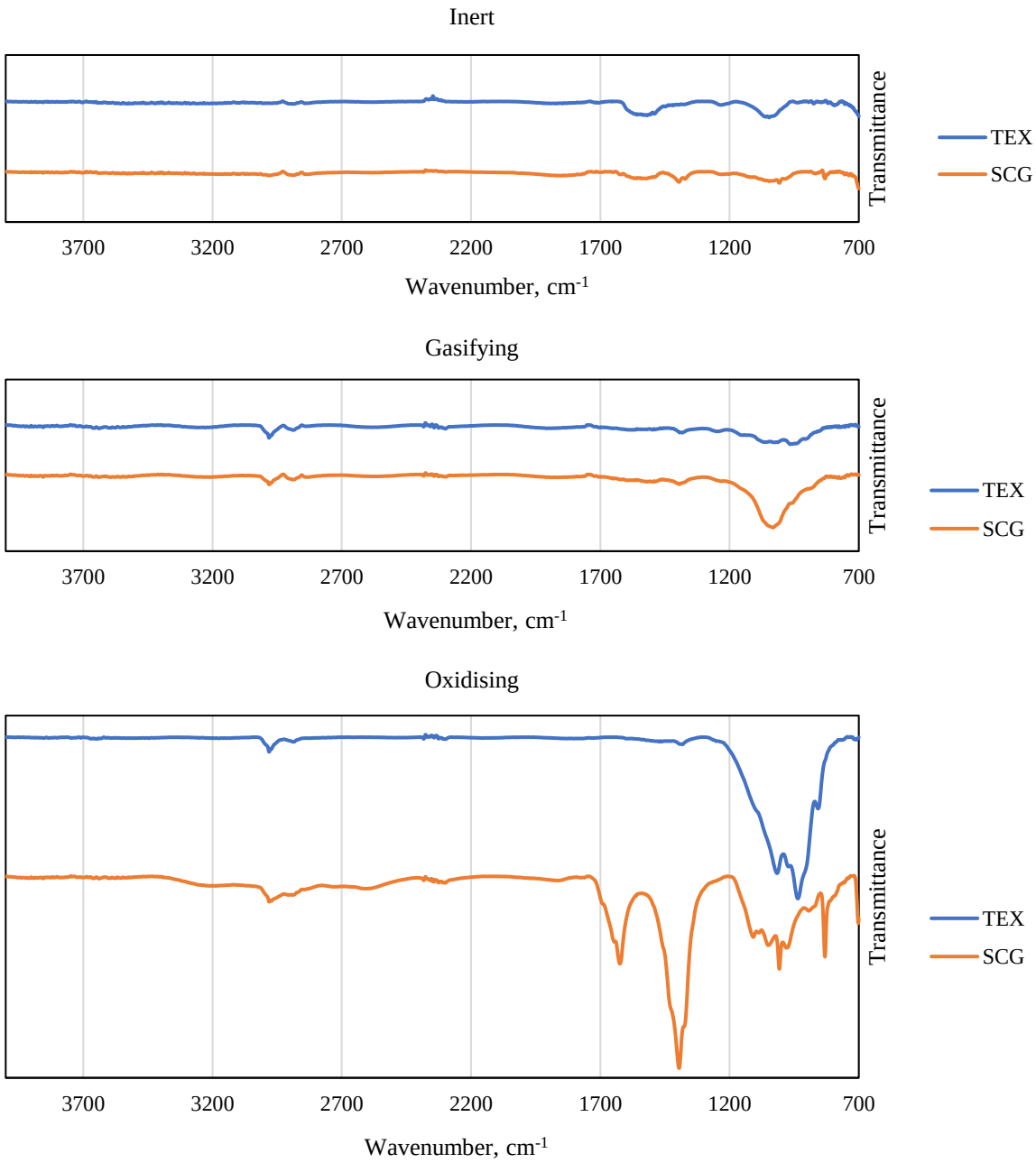

Figure 8. ATR-FTIR spectra of the solid residues from the textiles (TEX) and spent coffee grounds (SCG) conversion under inert, gasifying, and oxidising atmospheres

3.2 Characterisation of the pyrolytic char formed under different conditions

Thermal degradation under the inert atmosphere performed using lab-scale reactor in the slow and fast pyrolysis mode as well as muffle furnace (described in Section 2.2.1) resulted in the formation of residual pyrolytic chars abundant enough to be analysed with the gas adsorption method for surface area and pore size distribution calculations as well as with the thermogravimetric method for calculating the burning features and kinetic data.

3.2.1 Surface area and pore size distribution

The total surface area (S_total) and total pore volume (V_total) of the TEX and SCG chars were obtained using the dual two dimensional version of the non-local density functional theory (2D-NLDFT) model fitted simultaneously to the CO_2 and N_2 isotherms (Table 2). Incorporating CO_2 isotherm into the calculations allowed accounting for the micropores inaccessible to the nitrogen molecules, giving more accurate results. The specific surface area according to the Brunauer–Emmett–Teller (BET) method based on the N_2 isotherm was provided for an easier comparison with literature reports. Besides the cumulative values, the dual model was primarily used to approximate the pore size distribution (PSD) in chars (

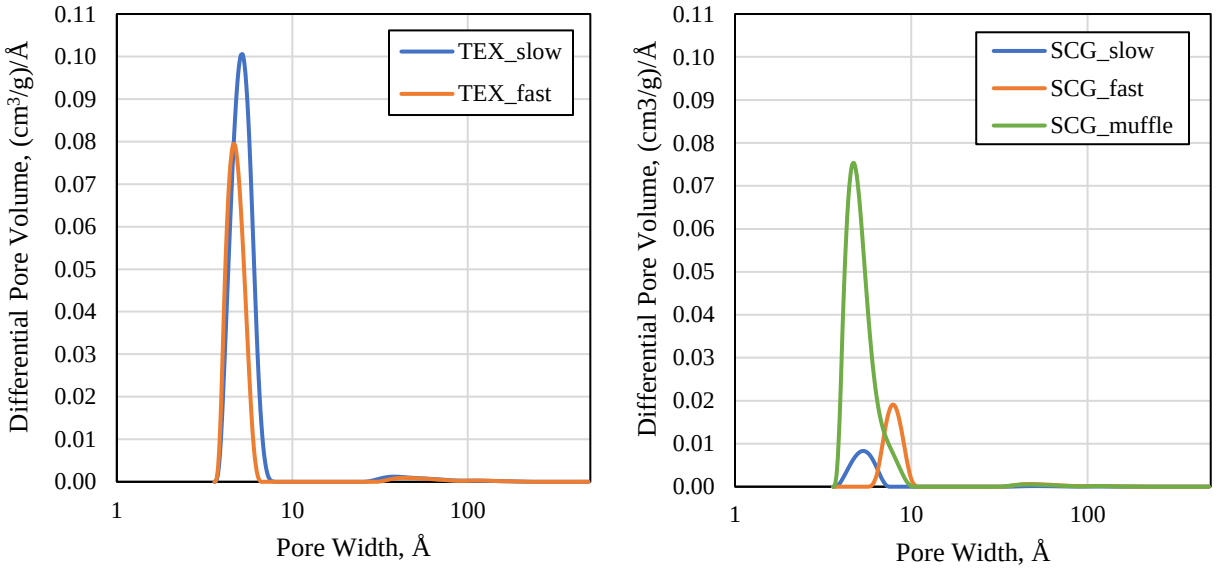

Figure 10).

The porosity of the TEX and SCG chars developed to a different extent, regardless of the pyrolysis conditions. Although microporous, the TEX chars from slow and fast pyrolysis possessed some larger pores that were able to facilitate N_2 molecules. On the other hand, the SCG char had extremally ultramicroporous structure – N_2 failed to enter the pores and even CO_2 adsorption was almost negligible (Figure 10). Most pores in the PSDs of microporous samples calculated with the dual model originate from the CO_2 measurement. Inclusion of the CO_2 isotherm is responsible for the dramatic difference between the total (S_total) and BET surface area of all examined chars, highlighting the importance of using appropriate probe molecules while examining microporous carbons [64].

The differences in the porosity of the TEX and SGS chars can be attributed to the properties of feedstock, as the same preparation conditions were applied during their preparation. The textiles are comprised of pure cellulose fibres, while spent coffee grounds have a substantial amount of

lignin, which is strongly cross-linked and more resistant to thermal degradation. Thus, in the case of SCG conversion, the development of the porosity of the cellulose residue was most likely hindered, as the escape of its volatiles was suppressed by the liquid derivatives of lignin decomposition, as observed by Chua et al. [65].

Highly microporous structure of the cellulose char has been previously reported, e.g. by Brunner et al. [66] where the surface areas in the range of 300-600 cm^2/g were calculated from the CO_2 adsorption while the calculation based on the N_2 isotherms estimated the specific surface of 1-5 m^2/g. Surface area of SCG chars as low as 1-1.5 m^2/g was evaluated with N_2 adsorption by Vardon et al. [67] and Stylianou et al. [68].

TEX char from fast pyrolysis developed significantly lower porosity compared to the slow process, as the high heating rate could hinder the release of volatiles [69]. In case of SCG, the increased porosity of the fast pyrolysis chars should be considered with caution; this sample had extremely low porosity and thus even CO_2 adsorption was extremely small, resulting in a poor fitting, which might have biased the PSD, as suggested by the unaccounted-for shift of the ultramicopore peak. Since the purely inert atmosphere yielded char that was de facto non-porous, the additional SCG pyrolysis test was performed in the muffle furnace using the closed-lid crucible, i.e., under highly depleted oxidiser concentration. This setup, although less controlled, might better reflect the conditions in the real combustion chamber. Indeed, the SCG char from the muffle furnace experiment developed more pores, suggesting that, despite the rapid volatiles release, some oxidising gases managed to access the surface of the sample.

Table 2 Total surface area (S_total) and pore volume (V_total) calculated from the dual 2D-NLDFT model and the BET surface area of the TEX and SCG chars from the slow, fast, and muffle furnace pyrolysis

	S_total, m^2/g	V_total, cm^3/g	BET, m^2/g
TEX_slow	710	0.243	81.1
TEX_fast	479	0.165	14.1
SGS_slow	65	0.025	0.9
SGS_fast	120	0.076	0.8
SGS_muffle	585	0.176	1.3

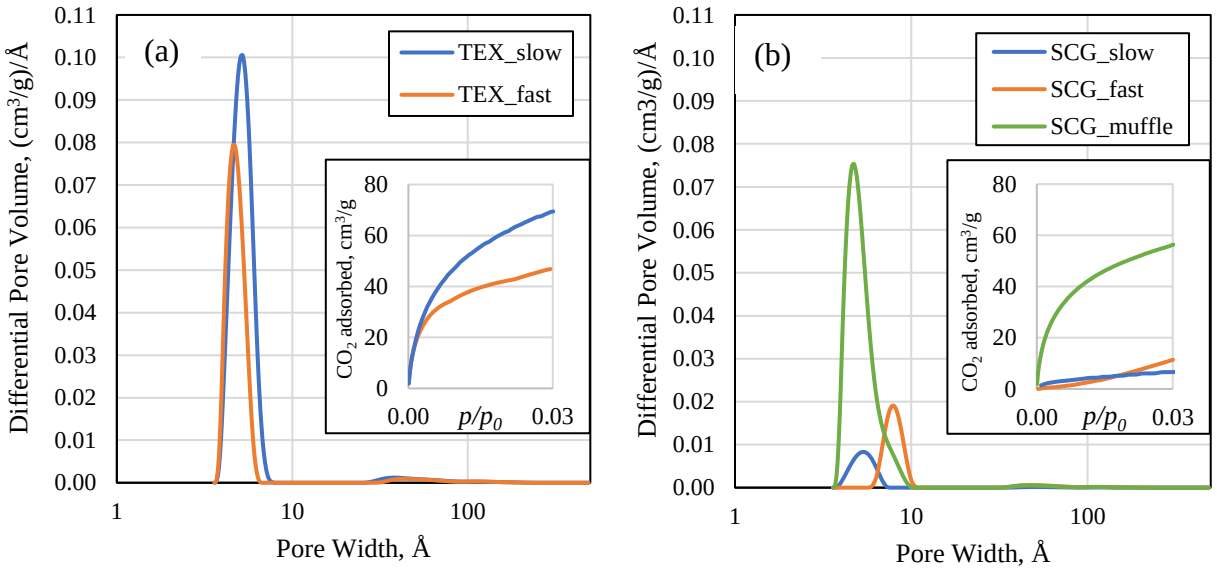

Figure 10. Pore size distribution (PSD) in (a) textile (TEX) and (b) spent coffee grounds (SCG) from slow and fast pyrolysis, and muffle furnace pyrolysis (CO_2 adsorption at 273 K showed in the small graph)

3.2.2 Thermal analyses

The thermogravimetric experimental results for the obtained chars are presented and compared by using thermogravimetric (TG) profiles and differential thermogravimetric (DTG) curves (Figs. 11–12). The features of the combustion acquired from the thermal analysis technique, summarised in Table 3, were used to effectively compare the reactivity and combustibility of chars resulting from the fast and slow pyrolysis of the selected waste (referred to as Fast TEX, Fast SCG, Slow TEX, and Slow SCG as appropriate).

Generally, it can be observed that the curve consists of one main mass loss, it can be ascribed to the combustion of char. During the oxidation char step, all the curves show a main peak that indicates the temperature corresponding to the maximum reaction rate. The maximum rate of weight loss in %/min during the main degradation process was Fast TEX (11.92) > Slow TEX (11.21) > Muffle furnace SCG (8.14) > Fast SCG (6.25) > Slow SCG (6.14). The lower maximum value of DTG and average weight loss rate for chars derived from SCG could be considered evidence of the low reactivity of lignin [70].

As presented, with an increased heating rate (β), DTG profiles shift to higher temperatures, and the rate of mass loss rises since the heat transfer is not as effective as it was for lower heating rates. It suggests that the degradation process is slower with the increasing of β that a higher heating rate causes the maximum combustion rate to be increased. The reason is the enhancement of mass transfer results from heat transfer intensification. This can be attributed to

the fact that the heating of solid particles occurs more gradually at lower heating rates, thus leading to an improved and more effective heat transfer to the inner part and among the particles. Similar findings were also observed in [25], [32], [40], [58].

Besides, as it can be seen, in all studied cases fast pyrolysis shifted the maximum peaks into lower temperatures and increased their values, for example, the maximum peak of TEX-char is 11.92 and 11.21 %/min at occurs at 537.5 and 541.9 °C for fast and slow pyrolysis, respectively. SCG-char sample maximum peak is 6.25 and 6.14 %/min and appears at the temperature of 513.4 °C and 574.9 °C for fast and slow pyrolysis, respectively. Interestingly, not only the reaction rate, but also the type of reactor is significant for the properties of biochar since the maximum peak of SCG-char derived from muffle furnace increased up to 8.14 %/min and took place at 470.4 °C.

For both, fast and slow pyrolysis, the ignition temperature (T_i) of char derived from SCG was lower than of that from textiles, namely, TEX_slow (475.4 °C) > SGS_slow (470.5 °C) and TEX_fast (469.6 °C) > SGS_fast (415.0 ° C). The fastest ignition occurred for SGC_muffle (400.1 °C). This indicates that both the SCG sample itself and the method of obtaining it, i.e. by fast pyrolysis, favour higher biochar reactivity.

Regarding combustion performance, firstly, we assessed the ignition index (D_i). As reported in Table 3, the heating rate of the pyrolysis process influenced the ignition index and the expected trend can be seen, namely the higher ignition index corresponds to the lower ignition temperatures within one material, for example, D_i of TEX_slow is lower than that of TEX_fast. Comparing two feedstocks, TEX and SCG, a different tendency has been observed, implying that the ignition index may not be the only factor to be concerned, related to the ignition temperature.

As Mureddu et al. [40] reported, it could be due to the higher content of ash in the sample, which can affect oxygen diffusion and heat transfer. This results in lower temperatures of ignition of SCG than that of the TEX-derived chars even if the ignition index of the TEX samples is higher than that of the SCG. The ignition index of the SCG-char produced in the muffle furnace was similar to TEX chars.

The values of S index for TEX-char samples are generally greater than SCG-char, meaning a better combustion performance of these samples. Comparing slow and fast pyrolysis, it can be noticed that higher heating rates result in char with superior combustion characteristics. Finally, the trend of H_f index follows the ignition and burnout indexes, showing smaller values for TEX-derived char samples, thus confirming their better combustion properties. Surprisingly, char derived from SCG pyrolysis in muffle furnace had the smallest value of H_f, which implies its high reactivity and intense combustion. C is adopted to evaluate the combustion stability of chars. The C indexes of the five kinds of chars are between 27.7×10^{-6} and 54.0×10^{-6}, among which the C index of TEX_fast is the highest, indicating that the combustion stability of this sample is the best.

Comparing the values of characteristic combustion parameters, such as Ti, S, C, and Hf, calculated in this work with values from the literature, it can be concluded that char derived from SGS_muffle has the properties most similar to coal [40], [71].

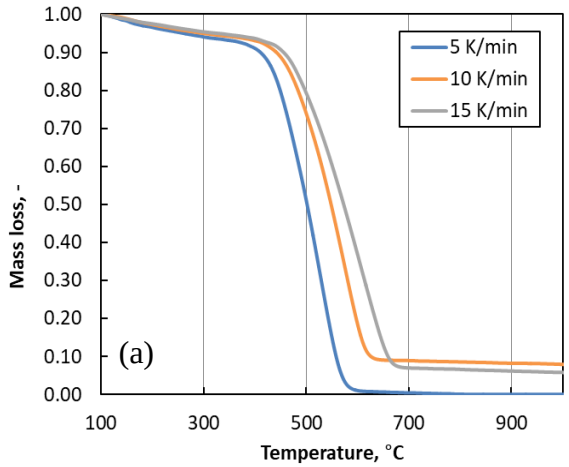

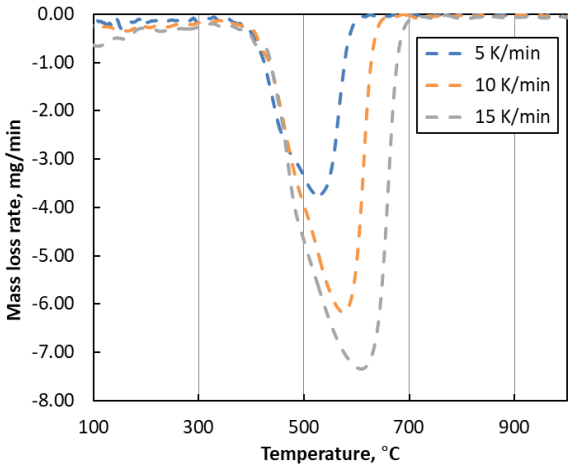

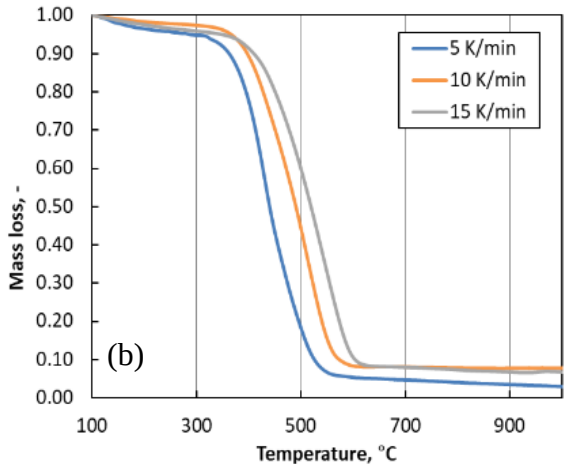

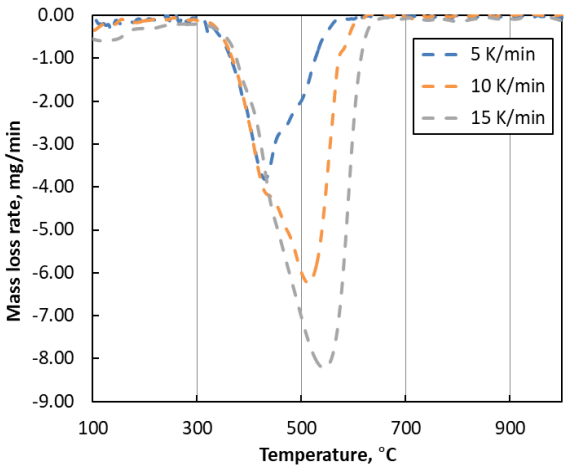

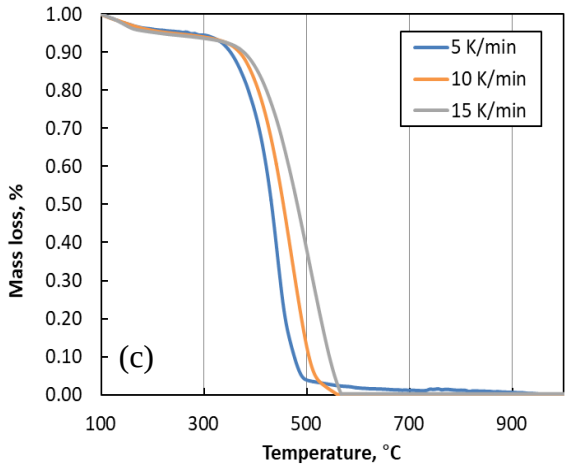

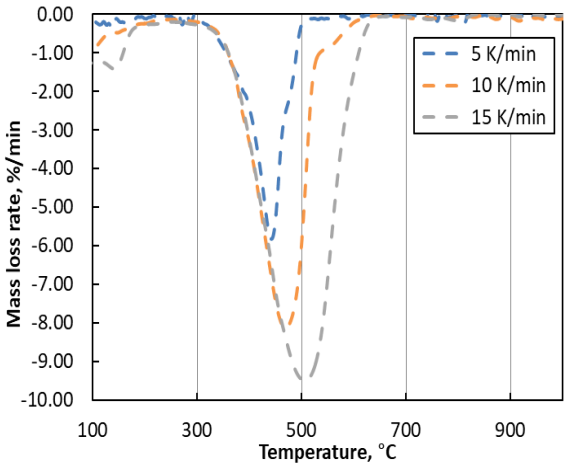

Figure 11. TG and DTG curves of char derived from spent coffee grounds a) slow, b) fast pyrolysis and c) fast pyrolysis in muffle furnace

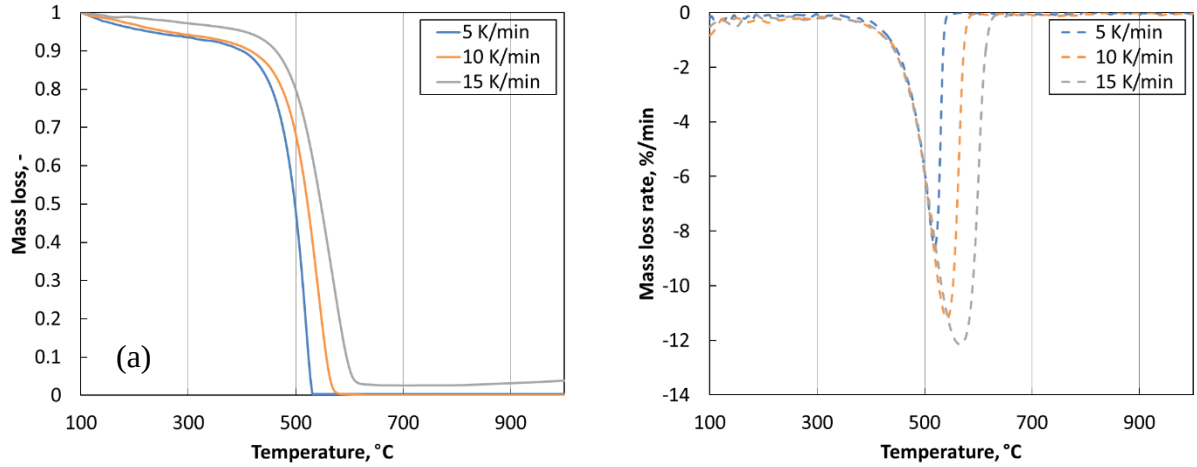

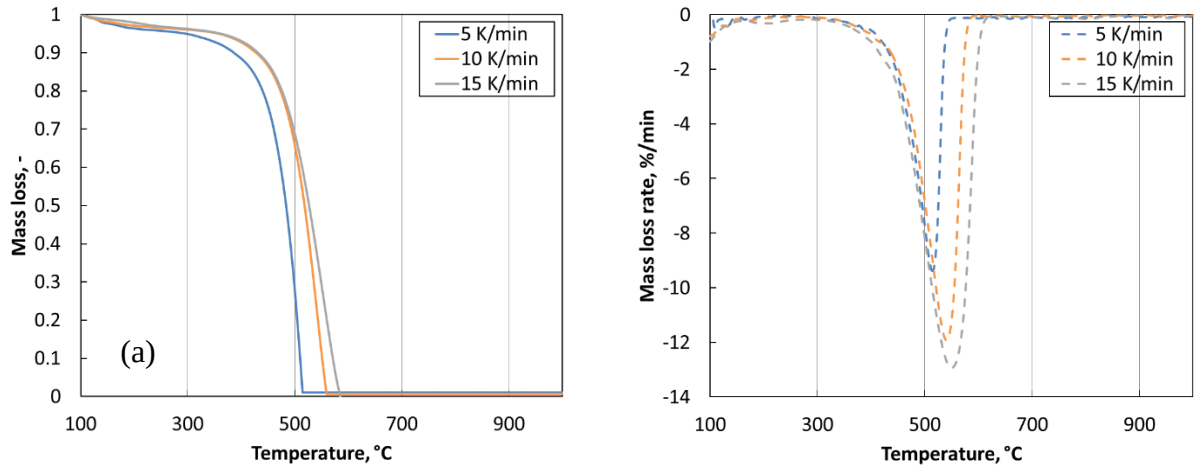

Figure 12. TG and DTG curves of char derived from textiles a) slow and b) fast pyrolysis

Table 3 Main oxy-combustion parameters of tested chars

Sample	SGS_slow	SGS_fast	SGS_muffle	TEX_slow	TEX_fast
Ignition Temperature, $°C$	470.5	415.0	400.1	475.4	469.6
Peak temperature, $°C$	574.9	513.4	470.4	541.9	537.5
Burnout temperature, $°C$	663.3	623.4	619.2	606.3	598.4
Ignition time, min	52.9	47.3	45.8	53.4	52.7
Peak time, min	63.5	57.3	52.9	60.1	59.7
Burnout time, min	72.5	68.3	67.4	66.8	65.8
DTG_{max}, $\%/min$	6.14	6.25	8.14	11.21	11.92
DTG_{mean}, $\%/min$	0.85	0.84	0.97	0.93	0.99
$\Delta t_{1/2}$, min	53.6	46.8	46.8	55.7	55.3
D_i, $wt.\%/min^3 \cdot 10^{-3}$	1.813	2.305	3.360	3.493	3.789
D_f, $wt.\%/min^4 \cdot 10^{-5}$	2.504	3.406	4.878	5.013	5.487
S, $wt.\%/(min^4 \cdot °C^2) \cdot 10^{-8}$	3.564	4.909	7.966	7.621	9.026
H_f, $°C \cdot 10^3$	3.750	2.148	1.844	2.055	2.002
C, $°C \cdot 10^{-6}$	27.736	36.290	50.850	49.601	54.053

3.2.3 Kinetic analysis

The isoconversional method can obtain more accurate apparent activation energy (Ea) without assuming the structure function f(x). In Tables 4-5, the average values of Ea and log(A) for SCG and TEX chars, respectively, are summarised. In this study, both Friedman's and Vyazovkin's methods yield similar results, which is consistent with our previous research [32].

Based on kinetic analysis, it was observed that in the case of SCG sample, higher heating itself did not have a strong influence on the activation energy of the char; it was slightly decreased by around 3 kJ/mol. However, char produced by using muffle furnace resulted in more reactive sample, and the value of Ea for SCG_muffle is 52 kJ/mol. As we stated before, it can be caused by the entry of oxygen into the furnace during the pyrolysis process, and thus more developed porosity and reactivity.

The larger differences can be observed in the case of TEX-derived chars. Increasing the heating rate resulted in higher Ea (kJ/mol), namely, TEX_fast (116.1) > TEX_slow (80.2). It can be also explained by the fact that slow pyrolysis developed significantly greater porosity compared to the fast devolatilization process.

Table 4 Kinetic parameters of oxy-combustion of SCG derived chars

Sample	SCG_slow		SCG_fast		SCG_muffle	
Method	Friedman	Vyazovkin	Friedman	Vyazovkin	Friedman	Vyazovkin
Average value of energy activation, kJ/mol	73.5	72.8	69.5	70.6	51.9	52.0
Average value of pre-exponential factor, Log(1/s)	2.162	2.104	2.057	2.144	1.130	1.173

Table 5 Kinetic parameters of oxy-combustion of TEX derived chars

Sample	TEX_slow		TEX_fast	
Method	Friedman	Vyazovkin	Friedman	Vyazovkin
Average value of energy activation, kJ/mol	80.2	80.1	116.1	116.4
Average value of pre-exponential factor, Log(1/s)	2.905	2.908	5.308	5.333

4. CONCLUSIONS

In this study, the thermal degradation of TEX and SCG in different atmospheres, i.e. inert, gasifying, and oxidising (with O_2/CO_2), was studied to evaluate the gas evolution profiles and analyse the solid residues. Additionally, chars derived from slow and fast pyrolysis were subjected to analysis. The results showed that shifting the atmosphere from inert to gasifying does not affect the thermal decomposition of samples below 600 °C. However, in the gasifying

atmosphere, the second peak of CO appears above 600 °C during the solid residue decomposition due to CO_2-char reactions. In the O_2/CO_2 atmosphere, the degradation of the solid residue occurs at lower temperatures and the immediate decomposition of volatiles can be observed due to the presence of the reactive oxygen. A similar share of carbon in the gaseous products was observed for gasification and oxidation test, suggesting nearly complete waste conversion.

Comparing the pyrolytic gas from the two materials, it can be concluded that the SCG sample yielded more calorific gas, which was richer in hydrogen and methane due to its more complex structure (larger amounts of hemicellulose and lignin).

The study shows the importance of the atmosphere during waste devolatilization and solid residue formation. The observed differences should be accounted for while modelling the WtE plants (including pyrolysis, gasification, and oxy- or air-incineration). Moreover, the residue formation under different atmospheres is an important aspect, since certain compounds in the ash can lead to corrosion and have a low temperature of melting point, for example, SiO_2 and K_2O, which leads to a requirement for costly cleaning and maintenance, and thus reduces the economic viability of the plant. These results also indicate that each group of waste should be investigated separately in order to create successful models of MSW utilisation technologies.

Regarding the properties of chars produced during the slow and fast pyrolysis of the investigated waste, it can be concluded that a higher heating rate resulted in chars with a lower porosity and, thus, lower reactivity: the study showed a direct correlation. The reason for this relationship can be that at a high heating rate, the release of volatiles could be hindered. Besides, SCG-chars were characterised by poorer developed pore structures than TEX-chars. However, as the study

proved, next to the heating rate, the method of sample preparation was important as well since SCG-chars prepared in a muffle furnace developed their specific surface better due to the possible access of oxygen in the process. Chars obtained from fast pyrolysis are characterised by superior combustion performance, lower temperature of ignition, higher maximum weight loss rates, and better stability.

This deep insight into the thermochemical conversion of waste, including the monitoring of gas evolution and product analysis, as well as the study of the combustion properties of the received chars under different conditions will provide a better understanding of these processes and aid the development of optimum routes for waste treatment.

ACKNOWLEDGMENTS

This research is supported by the National Science Centre (Project no. UMO-2021/41/N/ST8/02548) and Ministry of Education and Science (Poland) under statutory research funds of the Faculty of Energy and Environmental Engineering of SUT (08/060/RGZ200275-24). MD particiaption was funded by the Research Council of Norway through the ERANET Cofund ACT NEWEST-CCUS project (grant # 305062).

NOMENCLATURE

Abbreviations

C - flammability index

D_i - ignition index

D_f - burnout index

FTIR - Fourier-transform infrared spectroscopy

GC – Gas Chromatograph

H_f – stability index

MSW - Municipal Solid Waste

SCG – Spent Coffee Grounds

S – combustion activity index

TEX - Textiles

TGA - thermogravimetric analysis

WtE – Waste to Energy

β - Heating rate

REFERENCES

[1] K. Kaya, E. Ak, Y. Yaslan, and S. F. Oktug, "Sustainable Computing : Informatics and Systems Waste-to-Energy Framework : An intelligent energy recycling management," *Sustain. Comput. Informatics Syst.*, vol. 30, no. March, p. 100548, 2021, doi: 10.1016/j.suscom.2021.100548.

[2] L. Makarichi, W. Jutidamrongphan, and K. Techato, "The evolution of waste-to-energy incineration: A review," *Renew. Sustain. Energy Rev.*, vol. 91, pp. 812–821, Aug. 2018, doi: 10.1016/J.RSER.2018.04.088.

[3] R. Babu, P. M. P. Veramendi, and E. R. Rene, "Case Studies in Chemical and Environmental Engineering Strategies for resource recovery from the organic fraction of municipal solid waste," *Case Stud. Chem. Environ. Eng.*, vol. 3, no. March, p. 100098, 2021, doi: 10.1016/j.cscee.2021.100098.

[4] A. Kumar and S. R. Samadder, "A review on technological options of waste to energy for

effective management of municipal solid waste," *Waste Manag.*, vol. 69, pp. 407–422, 2017, doi: 10.1016/j.wasman.2017.08.046.

[5] S. Yi, Y. Jang, and A. K. An, "Potential for energy recovery and greenhouse gas reduction through waste-to-energy technologies," *J. Clean. Prod.*, 2018, doi: 10.1016/j.jclepro.2017.12.103.

[6] J. Dong, Y. Tang, A. Nzihou, and Y. Chi, "Key factors influencing the environmental performance of pyrolysis, gasification and incineration Waste-to-Energy technologies," *Energy Convers. Manag.*, vol. 196, no. May, pp. 497–512, 2019, doi: 10.1016/j.enconman.2019.06.016.

[7] E. N. Yargicoglu, B. Yamini, K. R. Reddy, and K. Spokas, "Physical and chemical characterization of waste wood derived biochars," *WASTE Manag.*, 2014, doi: 10.1016/j.wasman.2014.10.029.

[8] K. Weber and P. Quicker, "Properties of biochar," *Fuel*, vol. 217, no. January, pp. 240–261, 2018, doi: 10.1016/j.fuel.2017.12.054.

[9] L. Wang, T. Li, G. Várhegyi, Ø. Skreiberg, and T. Løvås, "CO2 Gasification of Chars Prepared by Fast and Slow Pyrolysis from Wood and Forest Residue: A Kinetic Study," *Energy and Fuels*, vol. 32, no. 1, pp. 588–597, 2018, doi: 10.1021/acs.energyfuels.7b03333.

[10] H. Abdullah and H. Wu, "Biochar as a fuel: 1. Properties and grindability of biochars produced from the pyrolysis of mallee wood under slow-heating conditions," *Energy and Fuels*, vol. 23, no. 8, pp. 4174–4181, 2009, doi: 10.1021/ef900494t.

[11] N. Pour, P. A. Webley, and P. J. Cook, "Potential for using municipal solid waste as a

resource for bioenergy with carbon capture and storage (BECCS)," *Int. J. Greenh. Gas Control*, vol. 68, pp. 1–15, 2018.

[12] Y. T. Tang, X. Q. Ma, Z. Y. Lai, and Y. Chen, "Energy analysis and environmental impacts of a MSW oxy-fuel incineration power plant in China," *Energy Policy*, vol. 60, pp. 132–141, 2013, doi: 10.1016/j.enpol.2013.04.073.

[13] B. J. P. Buhre, L. K. Elliott, C. D. Sheng, R. P. Gupta, and T. F. Wall, "Oxy-fuel combustion technology for coal-fired power generation," *Prog. energy Combust. Sci.*, vol. 31, no. 4, pp. 283–307, 2005.

[14] P. Wienchol, A. Szlęk, and M. Ditaranto, "Waste-to-energy technology integrated with carbon capture – Challenges and opportunities," *Energy*, vol. 198, p. 117352, May 2020, doi: 10.1016/j.energy.2020.117352.

[15] X. Li, V. Strezov, and T. Kan, "Energy recovery potential analysis of spent coffee grounds pyrolysis products," *J. Anal. Appl. Pyrolysis*, 2014, doi: 10.1016/j.jaap.2014.08.012.

[16] S. Kelkar *et al.*, "Pyrolysis of spent coffee grounds using a screw-conveyor reactor," *Fuel Process. Technol.*, vol. 137, pp. 170–178, 2015, doi: 10.1016/j.fuproc.2015.04.006.

[17] J. Pil, H. Seok, Y. Seok, H. Chae, and S. Joon, "Fast pyrolysis of coffee grounds : Characteristics of product yields and biocrude oil quality," *Energy*, vol. 47, no. 1, pp. 17–24, 2012, doi: 10.1016/j.energy.2012.06.003.

[18] A. Christou *et al.*, "Effects of biochar derived from the pyrolysis of either biosolids, manure or spent coffee grounds on the growth, physiology and quality attributes of field-grown lettuce plants," *Environ. Technol. Innov.*, vol. 26, p. 102263, 2022, doi: 10.1016/j.eti.2021.102263.

[19] D.-W. Cho *et al.*, "Adsorption of potentially harmful elements by metal-biochar prepared via Co-pyrolysis of coffee grounds and Nano Fe(III) oxides," *Chemosphere*, vol. 319, p. 136536, 2023, doi: https://doi.org/10.1016/j.chemosphere.2022.136536.

[20] Y. Kim, J. Lee, H. Yi, Y. Fai Tsang, and E. E. Kwon, "Investigation into role of CO2 in two-stage pyrolysis of spent coffee grounds," *Bioresour. Technol.*, vol. 272, pp. 48–53, 2019, doi: 10.1016/j.biortech.2018.10.009.

[21] D. W. Cho, J. Lee, K. Yoon, Y. S. Ok, E. E. Kwon, and H. Song, "Pyrolysis of FeCl3-pretreated spent coffee grounds using CO2 as a reaction medium," *Energy Convers. Manag.*, vol. 127, pp. 437–442, 2016, doi: 10.1016/j.enconman.2016.09.036.

[22] H. A. Kibret, Y.-L. Kuo, T.-Y. Ke, and Y.-H. Tseng, "Gasification of spent coffee grounds in a semi-fluidized bed reactor using steam and CO2 gasification medium," *J. Taiwan Inst. Chem. Eng.*, vol. 119, pp. 115–127, 2021, doi: https://doi.org/10.1016/j.jtice.2021.01.029.

[23] C. Primaz, O. Gil-Castell, and A. Ribes-Greus, "Strategies towards thermochemical valorisation of spent coffee grounds (SCG): Kinetic analysis of the thermal and thermo-oxidative decomposition," *Biomass and Bioenergy*, vol. 174, p. 106840, 2023, doi: https://doi.org/10.1016/j.biombioe.2023.106840.

[24] J. Fu *et al.*, "Co-circularity of spent coffee grounds and polyethylene via co-pyrolysis: Characteristics, kinetics, and products," *Fuel*, vol. 337, p. 127061, 2023, doi: https://doi.org/10.1016/j.fuel.2022.127061.

[25] C. Wen, Y. Wu, X. Chen, G. Jiang, and D. Liu, "The pyrolysis and gasification performances of waste textile under carbon dioxide atmosphere," *J. Therm. Anal.*

Calorim., vol. 128, no. 1, pp. 581–591, 2017, doi: 10.1007/s10973-016-5887-7.

[26] Y. Wu, C. Wen, X. Chen, G. Jiang, G. Liu, and D. Liu, "Catalytic pyrolysis and gasi fi cation of waste textile under carbon dioxide atmosphere with composite Zn-Fe catalyst," vol. 166, pp. 115–123, 2017, doi: 10.1016/j.fuproc.2017.05.025.

[27] Y. T. Tang, X. Q. Ma, Z. H. Wang, Z. Wu, and Q. H. Yu, "A study of the thermal degradation of six typical municipal waste components in CO2 and N2 atmospheres using TGA-FTIR," *Thermochim. Acta*, 2017, doi: 10.1016/j.tca.2017.09.009.

[28] N. Abdullah, R. Mohd, N. Syairah, M. Aziz, M. Rabie, and N. Disa, "Banana pseudo-stem biochar derived from slow and fast pyrolysis process," *Heliyon*, vol. 9, no. 1, p. e12940, 2023, doi: 10.1016/j.heliyon.2023.e12940.

[29] S. Al Arni, "Comparison of slow and fast pyrolysis for converting biomass into fuel," *Renew. Energy*, vol. 124, pp. 197–201, 2017, doi: 10.1016/j.renene.2017.04.060.

[30] G. Duman, C. Okutucu, S. Ucar, R. Stahl, and J. Yanik, "The slow and fast pyrolysis of cherry seed," *Bioresour. Technol.*, vol. 102, no. 2, pp. 1869–1878, 2011, doi: https://doi.org/10.1016/j.biortech.2010.07.051.

[31] M. M. Hasan, M. G. Rasul, and M. M. K. Khan, "The effects of slow and fast pyrolysis on the yields and properties of produced bio-oils from macadamia nutshell," *AIP Conf. Proc.*, vol. 2681, no. 1, 2022, doi: 10.1063/5.0114965.

[32] P. Wienchol, A. Korus, A. Szlęk, and M. Ditaranto, "Thermogravimetric and kinetic study of thermal degradation of various types of municipal solid waste (MSW) under N2, CO2 and oxy-fuel conditions," *Energy*, vol. 248, p. 123573, Jun. 2022, doi: 10.1016/J.ENERGY.2022.123573.

[33] Industrievereinigung Chemiefaser, "Production volume of chemical and textile fibers worldwide from 1975 to 2021," *Production volume of chemical and textile fibers worldwide from 1975 to 2021*. https://www.ivc-ev.de/sites/default/files/informationsmaterial-dateien/IVC Jahresbroschüre 2022.pdf (accessed Aug. 08, 2023).

[34] S. Yousef *et al.*, "A sustainable bioenergy conversion strategy for textile waste with self-catalysts using mini-pyrolysis plant," vol. 196, no. June, pp. 688–704, 2019, doi: 10.1016/j.enconman.2019.06.050.

[35] International Coffee Organization, "World coffee consumption," *World coffee consumption*, 2021. http://www.ico.org/prices/new-consumption-table.pdf (accessed Aug. 02, 2023).

[36] A. Korus *et al.*, "Kinetic parameters of petroleum coke gasification for modelling chemical-looping combustion systems," *Energy*, vol. 232, 2021, doi: 10.1016/j.energy.2021.120935.

[37] A. Korus, A. Samson, and A. Szlęk, "Catalytic conversion of toluene over a biochar bed under an inert atmosphere – The comparison of chars from different types of wood and the role of selected metals," *Fuel*, vol. 279, no. March, p. 118468, 2020, doi: 10.1016/j.fuel.2020.118468.

[38] B. G. Ma, X. G. Li, L. Xu, K. Wang, and X. G. Wang, "Investigation on catalyzed combustion of high ash coal by thermogravimetric analysis," *Thermochim. Acta*, vol. 445, no. 1, pp. 19–22, 2006, doi: 10.1016/j.tca.2006.03.021.

[39] J. J. Lu and W. H. Chen, "Investigation on the ignition and burnout temperatures of

bamboo and sugarcane bagasse by thermogravimetric analysis," *Appl. Energy*, vol. 160, no. 2015, pp. 49–57, 2015, doi: 10.1016/j.apenergy.2015.09.026.

[40] M. Mureddu, F. Dessì, A. Orsini, F. Ferrara, and A. Pettinau, "Air- and oxygen-blown characterization of coal and biomass by thermogravimetric analysis," *Fuel*, vol. 212, no. April, pp. 626–637, 2018, doi: 10.1016/j.fuel.2017.10.005.

[41] S. L. Niu, C. M. Lu, K. H. Han, and J. L. Zhao, "Thermogravimetric analysis of combustion characteristics and kinetic parameters of pulverized coals in oxy-fuel atmosphere," *J. Therm. Anal. Calorim.*, vol. 98, no. 1, pp. 267–274, 2009, doi: 10.1007/s10973-009-0133-1.

[42] L. Tang *et al.*, "Thermogravimetric Analysis of the Combustion Characteristics and Combustion Kinetics of Coals Subjected to Different Chemical Demineralization Processes," *ACS Omega*, vol. 7, no. 16, pp. 13998–14008, 2022, doi: 10.1021/acsomega.2c00522.

[43] B.-G. Ma, X.-G. Li, L. Xu, K. Wang, and X.-G. Wang, "Investigation on catalyzed combustion of high ash coal by thermogravimetric analysis," *Thermochim. Acta*, vol. 445, no. 1, pp. 19–22, 2006, doi: https://doi.org/10.1016/j.tca.2006.03.021.

[44] J. Chen *et al.*, "Co-combustion of sewage sludge and coffee grounds under increased O2/CO2 atmospheres: Thermodynamic characteristics, kinetics and artificial neural network modeling," *Bioresour. Technol.*, vol. 250, no. September 2017, pp. 230–238, 2018, doi: 10.1016/j.biortech.2017.11.031.

[45] M. Wilk, M. Śliz, and B. Lubieniecki, "Hydrothermal co-carbonization of sewage sludge and fuel additives: Combustion performance of hydrochar," *Renew. Energy*, vol. 178, pp.

1046–1056, 2021, doi: https://doi.org/10.1016/j.renene.2021.06.101.

[46] S. Vyazovkin *et al.*, “Thermochimica Acta ICTAC Kinetics Committee recommendations for collecting experimental thermal analysis data for kinetic computations,” vol. 590, pp. 1–23, 2014, doi: 10.1016/j.tca.2014.05.036.

[47] S. Vyazovkin, “Isoconversional kinetics of thermally stimulated processes,” *Springer*, 2015.

[48] S. Vyazovkin, A. K. Burnham, J. M. Criado, L. A. Pérez-maqueda, C. Popescu, and N. Sbirrazzuoli, “Thermochimica Acta ICTAC Kinetics Committee recommendations for performing kinetic computations on thermal analysis data,” *Thermochim. Acta*, vol. 520, no. 1–2, pp. 1–19, 2011, doi: 10.1016/j.tca.2011.03.034.

[49] J. Jagiello and J. P. Olivier, “2D-NLDFT adsorption models for carbon slit-shaped pores with surface energetical heterogeneity and geometrical corrugation,” *Carbon N. Y.*, vol. 55, no. 2, pp. 70–80, 2012, doi: 10.1016/j.carbon.2012.12.011.

[50] J. Jagiello, “Stable Numerical Solution of the Adsorption Integral Equation Using Splines,” *Langmuir*, vol. 10, no. 8, pp. 2778–2785, Aug. 1994, doi: 10.1021/la00020a045.

[51] T. Hosoya, H. Kawamoto, and S. Saka, “Pyrolysis gasification reactivities of primary tar and char fractions from cellulose and lignin as studied with a closed ampoule reactor,” *J. Anal. Appl. Pyrolysis*, vol. 83, no. 1, pp. 71–77, 2008, doi: 10.1016/j.jaap.2008.06.002.

[52] S. Sobek and S. Werle, “Solar pyrolysis of waste biomass: A comparative study of products distribution, in situ heating behavior, and application of model-free kinetic predictions,” *Fuel*, vol. 292, no. February, p. 120365, 2021, doi: 10.1016/j.fuel.2021.120365.

[53] C. Yue, P. Gao, L. Tang, and X. Chen, "Effects of N2/CO2 atmosphere on the pyrolysis characteristics for municipal solid waste pellets," *Fuel*, vol. 315, no. November 2021, p. 123233, 2022, doi: 10.1016/j.fuel.2022.123233.

[54] E. E. Kwon, S. Kim, and J. Lee, "Pyrolysis of waste feedstocks in CO2 for effective energy recovery and waste treatment," *J. CO2 Util.*, vol. 31, no. February, pp. 173–180, 2019, doi: 10.1016/j.jcou.2019.03.015.

[55] M. Ali, S. Yousef, J. Eimontas, and N. Stri, "Pyrolysis and gasification kinetic behavior of mango seed shells using TG-FTIR-GC-MS system under N2 and CO2 atmospheres," vol. 173, 2021, doi: 10.1016/j.renene.2021.04.034.

[56] W. Ma, G. Rajput, M. Pan, F. Lin, L. Zhong, and G. Chen, "Pyrolysis of typical MSW components by Py-GC / MS and TG-FTIR," *Fuel*, vol. 251, no. January, pp. 693–708, 2019, doi: 10.1016/j.fuel.2019.04.069.

[57] Q. Lu, X. Yang, C. Dong, Z. Zhang, X. Zhang, and X. Zhu, "Influence of pyrolysis temperature and time on the cellulose fast pyrolysis products : Analytical Py-GC / MS study," *J. Anal. Appl. Pyrolysis*, vol. 92, no. 2, pp. 430–438, 2011, doi: 10.1016/j.jaap.2011.08.006.

[58] S. Chen, A. Meng, Y. Long, H. Zhou, Q. Li, and Y. Zhang, "TGA pyrolysis and gasification of combustible municipal solid waste," *J. Energy Inst.*, vol. 88, no. 3, pp. 332–343, 2015, doi: 10.1016/j.joei.2014.07.007.

[59] O. Senneca, F. Cerciello, C. Russo, A. Wütscher, M. Muhler, and B. Apicella, "Thermal treatment of lignin , cellulose and hemicellulose in nitrogen and carbon dioxide," *Fuel*, vol. 271, no. March, p. 117656, 2020, doi: 10.1016/j.fuel.2020.117656.

[60] Y. Tang, X. Ma, Z. Lai, H. Lin, and J. Wu, "Char characteristics of municipal solid waste prepared under N2 and CO2 atmospheres," *J. Anal. Appl. Pyrolysis*, vol. 101, pp. 193–198, 2013, doi: 10.1016/j.jaap.2013.01.010.

[61] L. Wang, J. E. Hustad, Ø. Skreiberg, G. Skjevrak, and M. Grønli, "A critical review on additives to reduce ash related operation problems in biomass combustion applications," *Energy Procedia*, vol. 20, no. 1876, pp. 20–29, 2012, doi: 10.1016/j.egypro.2012.03.004.

[62] M. Criado, A. Fernández-Jiménez, and A. Palomo, "Alkali activation of fly ash: Effect of the SiO2/Na2O ratio: Part I: FTIR study," *Microporous Mesoporous Mater.*, vol. 106, no. 1–3, pp. 180–191, Nov. 2007, doi: 10.1016/J.MICROMESO.2007.02.055.

[63] D. H. Kim, K. Mudiyanselage, J. Szanyi, J. H. Kwak, H. Zhu, and C. H. F. Peden, "Effect of K loadings on nitrate formation/decomposition and on NOx storage performance of K-based NOx storage-reduction catalysts," *Appl. Catal. B Environ.*, vol. 142–143, pp. 472–478, Oct. 2013, doi: 10.1016/J.APCATB.2013.05.063.

[64] J. Jagiello, C. Ania, J. B. Parra, and C. Cook, "Dual gas analysis of microporous carbons using 2D-NLDFT heterogeneous surface model and combined adsorption data of N2 and CO2," *Carbon N. Y.*, vol. 91, pp. 330–337, 2015, doi: https://doi.org/10.1016/j.carbon.2015.05.004.

[65] Y. W. Chua, H. Wu, and Y. Yu, "Effect of cellulose–lignin interactions on char structural changes during fast pyrolysis at 100–350 °C," *Proc. Combust. Inst.*, vol. 38, no. 3, pp. 3977–3986, Jan. 2021, doi: 10.1016/J.PROCI.2020.08.014.

[66] P. H. Brunner and P. V. Roberts, "The significance of heating rate on char yield and char properties in the pyrolysis of cellulose," *Carbon N. Y.*, vol. 18, no. 3, pp. 217–224, Jan.

1980, doi: 10.1016/0008-6223(80)90064-0.

[67] D. R. Vardon *et al.*, "Complete utilization of spent coffee grounds to produce biodiesel, bio-oil, and biochar," *ACS Sustain. Chem. Eng.*, vol. 1, no. 10, pp. 1286–1294, Oct. 2013, doi: 10.1021/SC400145W/SUPPL_FILE/SC400145W_SI_001.PDF.

[68] M. Stylianou *et al.*, "Physicochemical and structural characterization of biochar derived from the pyrolysis of biosolids, cattle manure and spent coffee grounds," *J. Energy Inst.*, vol. 93, no. 5, pp. 2063–2073, Oct. 2020, doi: 10.1016/J.JOEI.2020.05.002.

[69] D. Angın, "Effect of pyrolysis temperature and heating rate on biochar obtained from pyrolysis of safflower seed press cake," *Bioresour. Technol.*, vol. 128, pp. 593–597, 2013, doi: https://doi.org/10.1016/j.biortech.2012.10.150.

[70] E. Garcia, I. F. Ejim, and H. Liu, "Thermogravimetric analysis of co-combustion of a bituminous coal and coffee industry by-products," *Thermochim. Acta*, vol. 715, p. 179296, 2022, doi: https://doi.org/10.1016/j.tca.2022.179296.

[71] Y. Yuan, Y. He, J. Tan, Y. Wang, S. Kumar, and Z. Wang, "Co-Combustion Characteristics of Typical Biomass and Coal Blends by Thermogravimetric Analysis," vol. 9, no. October, pp. 1–11, 2021, doi: 10.3389/fenrg.2021.753622.